

Exploring two different methods of seismic interpolating operators

Farzaneh Bayati and Daniel Trad

ABSTRACT

3D land data acquisitions are often undersampled along offset and azimuth directions because of large shot and receiver line intervals. In marine data acquisition, data are well sampled in the inline direction but coarsely sampled in the crossline direction. These issues can often be alleviated by seismic interpolation, which is an important step in data processing since many processing and migration tools require regularly sampled input data.

We compare two methods of seismic amplitude reconstruction. The first one is Singular Spectrum Analysis (SSA) which is based on rank reduction methods. In this approach, we generate Hankel matrices from constant frequency data and reduce their rank by using Truncated Singular Value Decomposition (TSVD). Since missing traces and random noise increase the rank of the Hankel matrix, TSVD changes the data by removing noise and interpolating missing traces. By reducing the rank, the algorithm iteratively infills missing traces. The second method is Minimum Weighted Norm Interpolation (MWNI) which infills missing traces by transforming the data to the Fourier domain and removing sampling artifacts by enforcing wavenumber-domain sparsity.

In this report, we test how these two methods perform on pre-stack and irregular sampled synthetic 2D data. For the case we tested, SSA seems more affected by curvature than MWNI but it seems better in preserving the amplitude for the hyperbola flanks. For SSA, we implement a multidimensional version and test it for 3D synthetic data.

INTRODUCTION

Reconstruction methods can be subdivided into wave-equation based and signal-processing based. Inside this second subdivision, most of the methods use transform domains such as Fourier which applies a prediction error filter in the $f - x$ domain.

Normally, 3D land data acquisitions have poor sampling for at least one of the spatial dimensions. In marine data acquisition, the data are well sampled in the inline direction and coarsely sampled in the crossline direction.

The objective of this paper is to compare the applications of Singular Spectrum Analysis (SSA) and Minimum Weighted Norm Interpolation (MWNI) to interpolate missing traces in regular and irregular patterns. SSA works in the $f - x$ domain of the data while relying on the rank reduction of the Hankel matrices. The interpolation algorithm uses an iterative algorithm applied by (Abma and Claerbout, 1995). On the other hand, MWNI works in $f - k$ domain by minimizing a wavenumber weighted norm that let us synthesize a prior spectral signature of the unknown wavefield.

Background

Singular Spectrum Analysis

Singular Spectrum Analysis (SSA) implemented with an iterative algorithm can interpolate seismic data, we can summarize the algorithm in 6 steps:

- 1- Transforming data from the time-space domain to the frequency-space.
- 2- Generating a Hankel matrix for each constant frequency.
- 3- Decomposition of the Hankel matrix in its singular spectrum via TSVD.
- 4- Rank reduction of the Hankel matrix.
- 5- Averaging in the Hankel matrix anti-diagonals.
- 6- Inverse Fourier transform to return to the time domain.

Let us consider a 2D seismic data in the time domain. which can be shown as:

$$S(x, t) = W(t - px), \quad (1)$$

where x defines the space, t is time, p is dip and $W(t)$ is the wavelet. To apply SSA, data are first transformed to the $f - x$ domain by a Fourier transform.

$$S(x, \omega) = A(\omega)e^{-i\omega px}, \quad (2)$$

where ω is the temporal frequency and A is the amplitude. For regular spacing, the spatial variable x is replaced by $x = n\Delta x$, and (Equation 2) becomes:

$$S(x, \omega) = A(\omega)e^{-i\omega pn\Delta x}. \quad (3)$$

Equation 3 can be used for the previous channel as follows:

$$S_{n-1} = A(\omega)e^{-i\omega p(n-1)\Delta x} = A(\omega)e^{-i\omega pn\Delta x}e^{i\omega p\Delta x}. \quad (4)$$

From comparing Equation 2 and Equation 3 we see that the channel S_n is related to the previous channel S_{n-1} :

$$S_n = PS_{n-1}, P = e^{i\omega p\Delta x}. \quad (5)$$

Equation 5 shows a linear recursion between adjacent channels that represents the predictability of the signal in the $f - x$ domain (Sacchi and Kuehl, 2001; Ulrych and Sacchi, 2005). This predictability is the key element in the success of SSA for random noise attenuation and missing traces interpolation.

Continuing to step (2) let us consider $S_\omega = [s_1, s_2, s_3, \dots, s_{N_x}]^T$, a spatial vector of a constant frequency in the $f - x$ domain, where N_x is the number of space samples of the data. Embedding of each frequency into a Hankel matrix is as follows:

$$M = \begin{pmatrix} s_1 & s_2 & \dots & s_{k_x} \\ s_2 & s_3 & \dots & s_{k_x+1} \\ \vdots & \vdots & \ddots & \vdots \\ s_{L_x} & s_{L_x+1} & \dots & s_{N_x} \end{pmatrix}, \quad (6)$$

where K_x and L_x control the dimension of the Hankel matrix. It is recommended to use a square Hankel matrix for the SSA algorithm (Trickett, 2008). Substituting Equation 5 into

Equation 6, the following linear relationship between the columns of the Hankel matrix arise:

$$M = \begin{pmatrix} s_1 & P s_1 & \dots & P^{K_x-1} s_1 \\ s_2 & P s_2 & \dots & P^{K_x-1} s_2 \\ \vdots & \vdots & \ddots & \vdots \\ s_{L_x} & P s_{L_x} & \dots & P^{K_x-1} s_{L_x} \end{pmatrix}. \quad (7)$$

From Equation 7 we can find that the rank of the Hankel matrix in the $f - x$ domain for a signal without any noise will be 1. In the presence of random noise or missing traces, the rank of the Hankel matrix will increase (Figure 1).

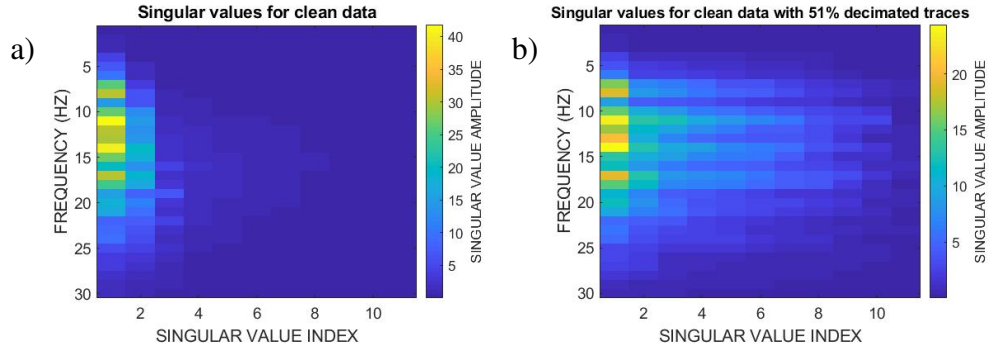


FIG. 1. a) Singular values for noiseless data without decimated traces; b) singular values for noiseless data with 51% decimated traces.

The singular value decomposition of the Hankel matrix M is written as:

$$svd(M) = U \Sigma V^H, \quad (8)$$

where Σ is a diagonal matrix of singular values for the matrix M , and U and V are the orthogonal matrices of singular vectors of the matrix M (Golub and Reinsch, 1971).

$$U U^H = V^H V = V V^H = I_n, \quad (9)$$

$$\Sigma = \text{diag}(\sigma_1, \dots, \sigma_n), \quad (10)$$

where σ_i are the singular values and the number of non-zero singular values in the Hankel matrix determines the rank of the Hankel matrix. The goal of SSA is to reduce the rank of the Hankel matrix. We can obtain the reduced rank matrix as follow:

$$M_k = U_k \Sigma_k V_k^H, \quad (11)$$

where Σ_k is a diagonal matrix containing the k largest singular values of M , U_k and V_k are the k first singular vectors of the matrix M . By averaging the anti diagonals of each Hankel matrix the matrix M can be obtained. This procedure, truncated SVD, will eliminate random noise from the data. The interpolation problem, reconstructing missing traces, requires more sophistication. Lets go back to Equation 6 and consider it with missing traces. For example, let us consider the signal S in the frequency slice with $N_x = 9$ and some

missing traces as $S_\omega = [s_1, 0, s_3, 0, s_5, s_6, s_7, 0, 0]^H$. The Hankel matrix of S_ω will be as follows:

$$M = \begin{pmatrix} s_1 & 0 & s_3 & 0 & s_5 \\ 0 & s_3 & 0 & s_5 & s_6 \\ s_3 & 0 & s_5 & s_6 & s_7 \\ 0 & s_5 & s_6 & s_7 & 0 \\ s_5 & s_6 & s_7 & 0 & 0 \end{pmatrix}. \quad (12)$$

Let us define a sampling operator which is 1 for each observed component and 0 for zero values. This means $T(i) = 1$ for nonzero components and $T(i) = 0$ for the missing traces. The processes of reconstructing and denoising for each frequency can be written as follows:

$$S_f^i = S_f^{obs} + (I - T) \odot F_{SSA} S_f^{i-1}, \quad i = 1, 2, \dots \quad (13)$$

where i is the iteration, f denotes the constant frequency we are applying SSA, $I = \text{ones}(\text{size}(T))$, the operator \odot is the array multiplication for two matrices, and F_{SSA} is the function of the SSA application. The algorithm stops either when the maximum number of iterations is reached, or the energy of change in the recovered traces is less than a threshold (Oropeza and Sacchi, 2011).

Equation 13 works well for noiseless data. To recover amplitudes of a noisy data Oropeza and Sacchi (2011) proposed a modification of the iterative algorithm:

$$S_f^i = \alpha^i S_f^{obs} + (1 - \alpha^i) T \odot F_{SSA} S_f^{i-1} + (I - T) \odot F_{SSA} S_f^{i-1}, \quad i = 1, 2, \dots, \quad (14)$$

where α is an iteration-dependent scalar that linearly decreases from $\alpha^1 \simeq 1$ to $\alpha^{pmax} = 0$. It causes the gradual embedding of the filtered data to the original data.

SSA can easily be expanded to more than two dimensions, which is called multidimensional singular spectrum analysis (MSSA). The expansion of SSA to two spatial dimensions and one temporal dimension is the same as the SSA algorithm but it has one step more. The steps of MSSA is summarized as below:

- 1- Transforming data from t-x-y to f-x-y.
- 2- Generating Hankel matrices in one of the spatial dimensions in a constant frequency.
- 3- Embedding the generated Hankel matrices into block of Hankel matrix for each frequency.
- 4- Decomposition of the block Hankel matrix in its singular spectrum via TSVD.
- 5- Rank reduction of the block of Hankel matrix.
- 6- Averaging in the block Hankel matrix anti-diagonals.
- 7- Inverse Fourier transform to return to the time domain.

The iterative algorithm of Equation 13 together with the above steps can infill missing traces for 3D data, provided that the events in the data are approximately linear.

Minimum Weighted Norm Interpolation

Minimum Weighted Norm Interpolation (MWNI) is designed to work in the $(f - x)$ and $(f - k)$ Fourier domains. The algorithm works with one frequency slice at a time. Let us consider the signal in Equation 2, $S_\omega = [s_1, s_2, \dots, s_{N_x}]^T$, and the sampling operator T . The complete data and the observed data are connected by a linear system:

$$d = LS. \quad (15)$$

As an example of a signal with $N_x = 9$ and some missing traces like $S_\omega = [s_1, 0, s_3, 0, s_5, s_6, s_7, 0, 0]^T$ we can show:

$$\begin{pmatrix} s_1 \\ s_3 \\ s_5 \\ s_6 \\ s_7 \end{pmatrix} = \begin{pmatrix} 1 & 0 & 0 & 0 & 0 & 0 & 0 & 0 & 0 \\ 0 & 0 & 1 & 0 & 0 & 0 & 0 & 0 & 0 \\ 0 & 0 & 0 & 0 & 1 & 0 & 0 & 0 & 0 \\ 0 & 0 & 0 & 0 & 0 & 1 & 0 & 0 & 0 \\ 0 & 0 & 0 & 0 & 0 & 0 & 1 & 0 & 0 \end{pmatrix} (s_1, s_2, s_3, s_4, s_5, s_6, s_7, s_8, s_9)^T. \quad (16)$$

Solving Equation 15 leads to an undetermined system of equations. Among all the possible solutions, MWNI chooses a solution which minimizes a model norm. The inversion can be reduced to solving the constrained minimization problem:

minimizing $\|S\|_p^2$ subjects to $LS = d$, where $\|\cdot\|_p$ indicates a weighted norm. In the presence of noise, the above constraints can be modified as: Minimize $\|W_s S\|_p^p$ subject to $\|W_d(d - LS)\|_q^q = \phi_d$, where p and q indicate the different norms used to estimate the size of the quantities involved, ϕ_d is the estimation of noise plus a residual due to the failure of the model, W_s is a matrix of model weights and W_d is a matrix of data weights. To obtain the desired solution we should minimize the cost function:

$$(\lambda W_s^T W_s + L^T W_d^T W_d L)S = L^T W_d^T W_d d, \quad (17)$$

where λ is a trade-off parameter. Equation 15 is solved by fixing the model to some previous estimation (like the spatial spectra from the previous temporal frequency) and applying a linear minimization by conjugate gradient algorithm (CG). To prevent a potential zero division (for a zero model) we can apply right preconditioning:

$$d = L W_s^{-1} W_s S, \quad (18)$$

with $W_s S$ being a new model \tilde{S} , and $L W_s^{-1}$ being a new operator \tilde{L} . The optimization problem leads to: Minimize $\|\tilde{S}\|_p^p$ subject to

$$\|W_d(d - L W_s^{-1} \tilde{S})\|_q^q = \phi_d. \quad (19)$$

The following system is the result of the minimization of the cost function of Equation 19:

$$(\lambda I + W_s^{-T} L^T W_d^T W_d L W_s^{-1})\tilde{S} = W^{-T} T_s. \quad (20)$$

Equation 20 is solved by setting the trade-off parameter to 0 and letting the number of internal iterations in the conjugate gradient play the role of regularizer (Trad, 2003). The FFT algorithm assumes data are regular so binning is needed before applying the algorithms for interpolation (Liu and Sacchi, 2004) and (Trad, 2009).

Results and discussions

To compare SSA results with MWNI we present several tests. SSA and MWNI are tested on a synthetic data set with different hyperbolic events sparseness. To compare the quality of data (Q) we use Equation 21.

$$Q = 10 \log_{10} \left(\frac{\|d_0\|_2^2}{\|d_f - d_0\|_2^2} \right), \quad (21)$$

where d_0 is the result after applying interpolation algorithms and d_f is the expected data. This allows us to test the accuracy of the results numerically.

Example 1

The first 2D synthetic pre-stack dataset tested contains three hyperbolic events with different curvatures and 95 traces, of which 30% are zeroes. The data quality for input data is 3.14 *dB*, and the output data quality for the SSA algorithm is 19.49 *dB* and for MWNI is 18.26 *dB*. To assume that the input data is linear in the SSA algorithm, we set the size of input spatial windows to 25 of which 12 traces overlap. The best rank for the Hankel matrix is set to 3 for each frequency, and the algorithm converges after 7 iterations. Figure 2 shows the results of applying SSA and MWNI algorithms. We observe that both algorithms almost successfully recover the missing traces, and the coherency of the events is maintained (Figure 2-c and 2-e). The differences between the interpolated results and the expected are shown in (Figure 2-d and 2-f).

Example 2

To analyse whether the algorithms can recover missing traces for more sparse data, we randomly zeroed 51% traces. Figure 3 shows that both methods give comparable results. Input data quality is -0.15 *dB*. And the output data quality for the SSA algorithm is 10.40 *dB*, whereas it is 12.45 *dB* for MWNI. For the SSA algorithm, we select 25 traces for the size of input spatial windows, of which 20 overlap. We choose the rank of the Hankel matrix to 3, for which the algorithm converged after 7 iterations. The results of interpolation for SSA and MWNI algorithms are shown in Figure 3. We can observe that the coherency of the events is maintained, but the amplitudes are not completely recovered (Figure 3-c and 3-e). The residuals results from both algorithms are shown in (Figure 3-d and 3-f).

Example 3

In the real world of seismic data acquisition, it is hard to maintain the survey in a regular pattern because of logistic constraints and economic restrictions. Many of the seismic processing and imaging methods such as pre-stack migration and fracture analysis, often need the data to be regularly spaced. The simplest method to handle seismic data irregularity is called "binning". The binning errors are kept small by applying normal move out (NMO) and static corrections before interpolation (Trad, 2009). Also, NMO improves the lateral correlation of events reducing the region of support in the $f - k$ domain, making model weights to change slow with frequency.

In Figure 4 we see results of applying SSA and MWNI to an irregularly sampled synthetic data set with three events. Quality of the input data is 6.92 *dB*. And the output data quality for the SSA algorithm is 10.45 *dB*, whereas it is 11.12 *dB* for MWNI. Both algorithms apply a binning to set regular grids.

Example 4

So far we discussed the results of SSA and MWNI in 2 dimensions. In this example, we create a seismic cube with 3 dimensions, 2 spatial and time, to analyse the behaviour of SSA in 3D (Figure 5). 51% of the traces are randomly killed. Input data quality is 0.23 *dB*. We set small spatial windows of 33×11 and the rank $k = 4$. The algorithm converged after 3 iterations with an output data quality of 10.30 *dB*. Figure 6 shows the interpolation results for an inline of the data cube at $y=5$.

Example 5

To simulate the real data conditions, we tested a 3D shot with irregular receiver locations, and binned the traces in a regular grid with cell size of 100×10 (Figure 7 and 8). When binning, some cells contain more than one trace while others remain empty. The cells containing several traces are averaged to obtain only one trace. Figure 9 is a slice of the 3D cube at $y=5$.

Example 6

In this example, we test the capability of the MSSA algorithm for noisy data reconstruction. Figure 10 shows the same 3D cube from example 4 but this time contaminated with random noise giving a data quality of 1.06 *dB*. When setting the rank of the block Hankel matrix to $k = 4$, the algorithm converged after 8 iterations and input data quality of 5.48 *dB*. Figure 11 shows a slice of the data cube at $y=2$.

Example 7

The proposed iterative algorithm for SSA does not work well for regularly decimated traces. For this case, we tried to perform interpolation of the Hankel matrix eigenvectors. This was successful only for very simple data. By fitting a polynomial to the nonzero components of the eigenvectors, we could create the equivalent eigenvectors for the complete data. Figure 12 depicts the result of this approach for SSA, the MWNI result, and their $f - k$ spectrums. MWNI has dealiased and recovered the data completely while there are still some artefacts remaining on SSA results.

Summary and discussion

In this paper, we have compared two methods of seismic interpolation: singular spectrum analysis (SSA), which depends on the rank reduction of the Hankel matrix via truncated SVD, and minimum weighted norm interpolation (MWNI) that minimizes a wavenumber weighted norm. Synthetic pre-stack 2D data examples indicate that both algorithms recover the amplitude nearly completely. SSA with an iterative algorithm recovered well the amplitude of irregular and coarsely sampled data, but it did not work well on our example with regularly decimated data. On the other hand, MWNI interpolated well the regularly decimated data when using a FK filter mask. Results for MWNI can be improved by using finer binning and more dimensions (3D, 4D or 5D interpolation). For SSA we couldn't

improve the results with finer binning but it would probably get better for more than 3 dimensions. Some parameters are required for both algorithms. The number of iterations, the rank of the Hankel matrix, which is related to the number of the dips in each window and the window size. The rank of the Hankel matrix is a trade-off parameter. For the SSA algorithm, we find the size of the spatial windows is very important. It has to be small enough such that we only have mostly linear events leading to a small rank. However, if too small, then there are not enough information to interpolate.

Acknowledgments

We thank the sponsors of CREWES for continued support. This work was funded by CREWES industrial sponsors, and NSERC (Natural Science and Engineering Research Council of Canada) through the grant CRDPJ 461179-13.

REFERENCES

- Abma, R., and Claerbout, J., 1995, Lateral prediction for noise attenuation by tx and fx techniques: *Geophysics*, **60**, No. 6, 1887–1896.
- Golub, G. H., and Reinsch, C., 1971, Singular value decomposition and least squares solutions, *in* *Linear Algebra*, Springer, 134–151.
- Liu, B., and Sacchi, M. D., 2004, Minimum weighted norm interpolation of seismic records: *Geophysics*, **69**, No. 6, 1560–1568.
- Oropeza, V., and Sacchi, M., 2011, Simultaneous seismic data denoising and reconstruction via multichannel singular spectrum analysis: *Geophysics*, **76**, No. 3, V25–V32.
- Sacchi, M. D., and Kuehl, H., 2001, Arma formulation of fx prediction error filters and projection filters: *Journal of Seismic Exploration*, **9**, No. 3, 185–198.
- Trad, D., 2003, Interpolation and multiple attenuation with migration operators: *Geophysics*, **68**, No. 6, 2043–2054.
- Trad, D., 2009, Five-dimensional interpolation: Recovering from acquisition constraints: *Geophysics*, **74**, No. 6, V123–V132.
- Trickett, S., 2008, F-xy cadzow noise suppression, *in* *SEG Technical Program Expanded Abstracts 2008*, Society of Exploration Geophysicists, 2586–2590.
- Ulrych, T. J., and Sacchi, M. D., 2005, *Information-based inversion and processing with applications*, vol. 36: Elsevier.

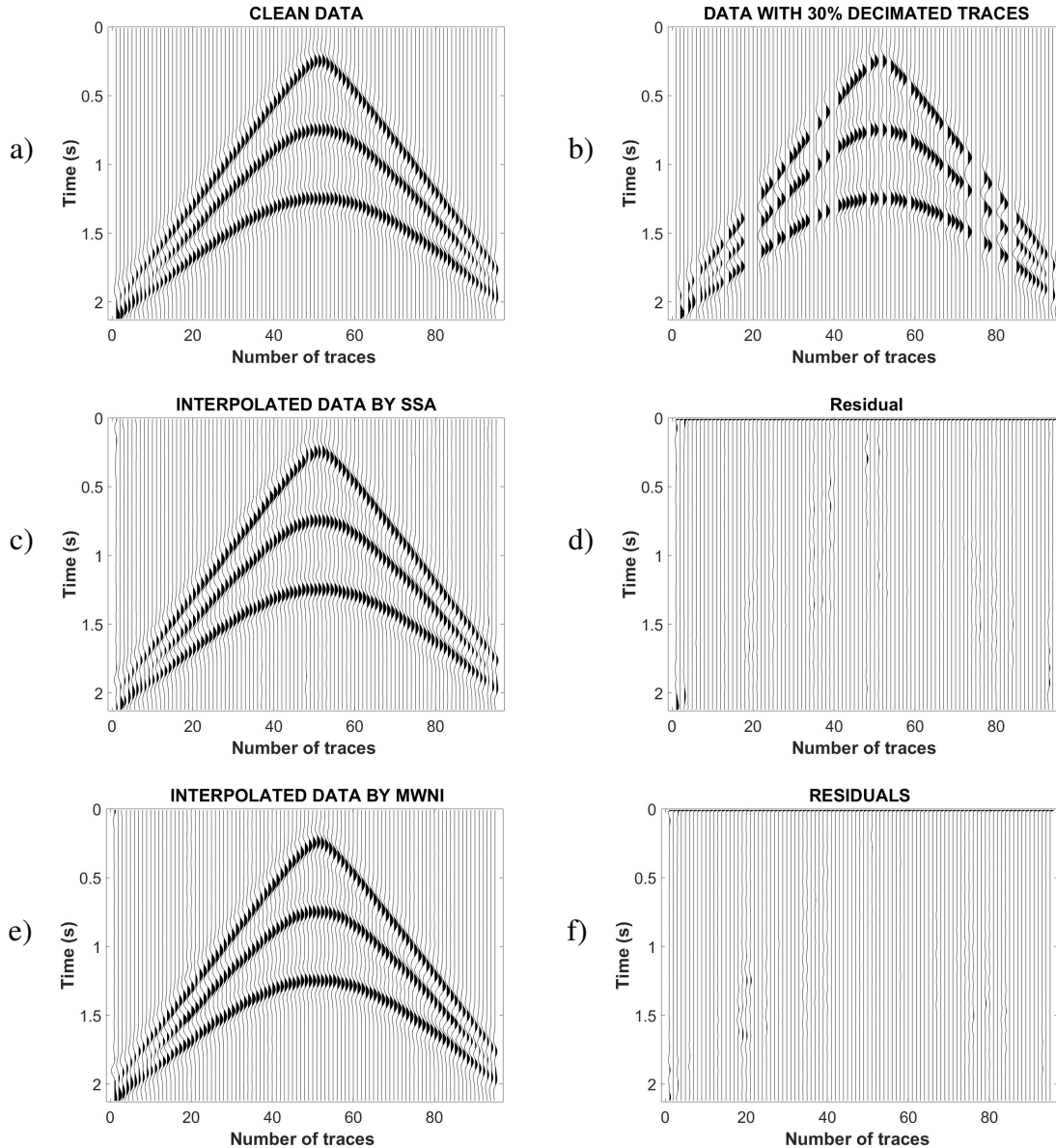


FIG. 2. Comparison between the SSA and MWNI algorithms applied to the 2-D pre-stack synthetic noiseless data having 3 different curved events and 30% decimated traces. a) Clean data prior to killing traces; b) input data with 30% zeroed traces; c) result of applying SSA; d) difference between clean data and interpolated data from applying SSA; e) result of MWNI interpolation; f) difference between clean data and interpolated data from applying MWNI.

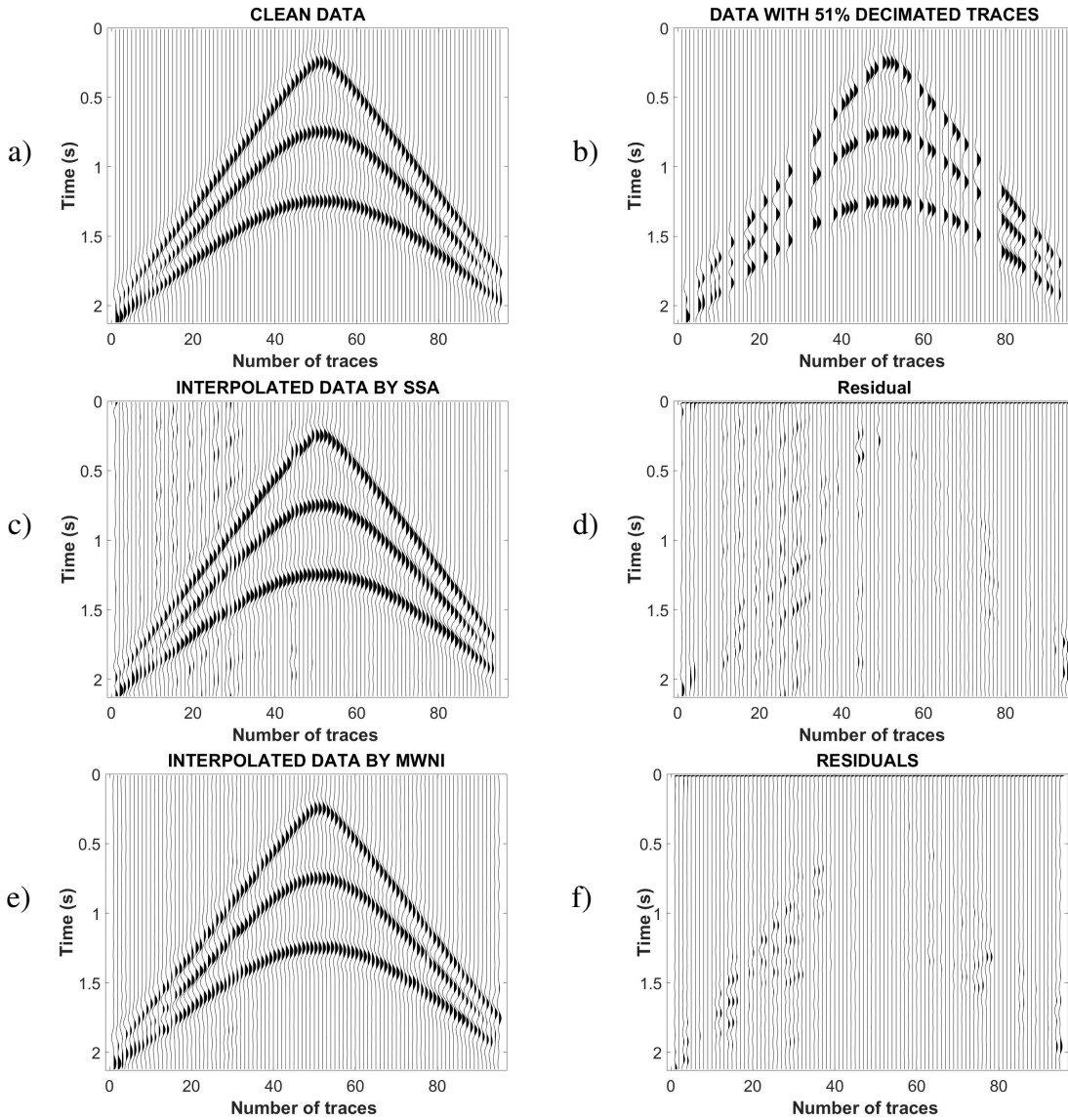


FIG. 3. Comparison between SSA and MWNI algorithms applied on 2-D pre-stack synthetic noiseless data with 3 different hyperbolic events and 51% decimated traces. a) Clean data prior to killing traces; b) input data with 51% randomly killed traces; c) SSA interpolation result; d) difference between clean data and SSA result; e) MWNI interpolation result; f) difference between clean data and MWNI result.

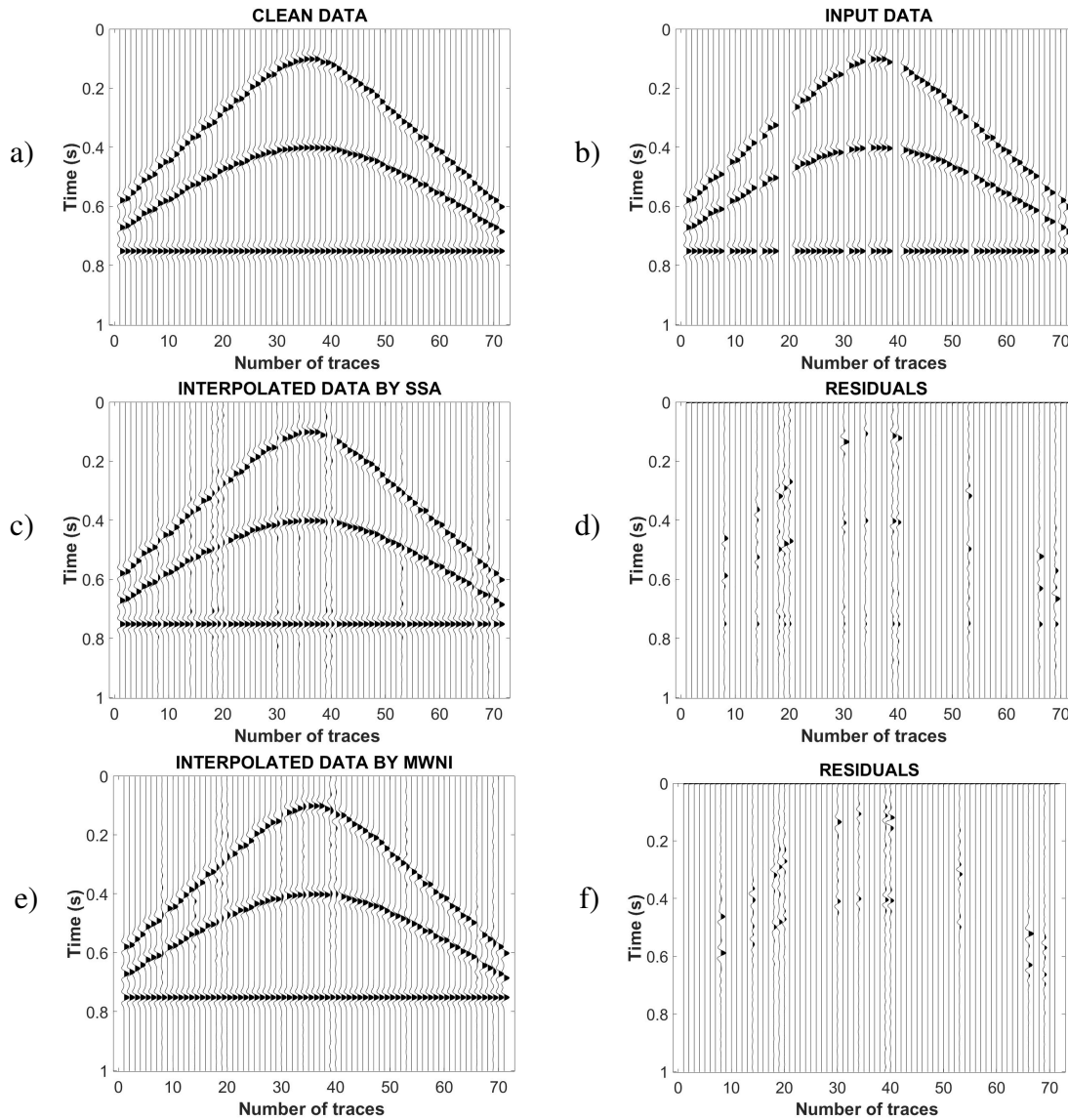


FIG. 4. Comparison between SSA and MWNI algorithms applied on 2-D irregular pre-stack synthetic noiseless data with 3 different curved events and 20% randomly decimated traces. a) Clean data prior to killing traces; b) input data with 20% randomly decimated traces; c) reconstruction using SSA; d) difference between clean data and interpolated data by SSA; e) reconstruction using MWNI; f) the difference between clean data and interpolated data by MWNI.

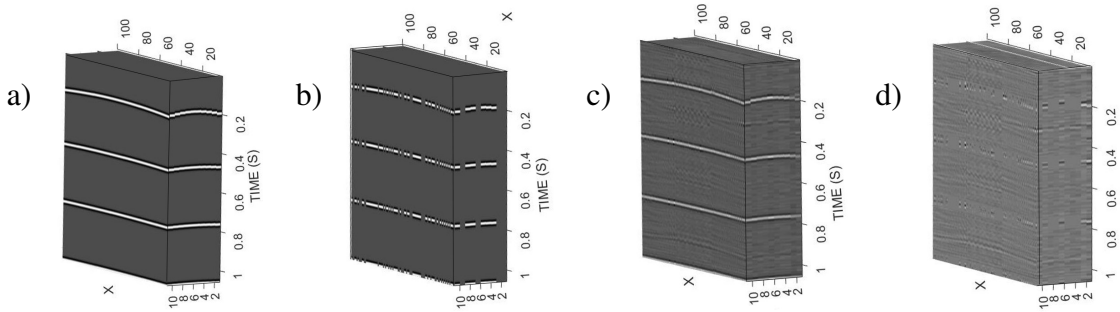


FIG. 5. Interpolation of a pre-stack synthetic cube presenting 4 events. a) Initial data; b) input data with 51% randomly killed traces; c) result of the interpolation using MSSA; d) difference between the result and initial data.

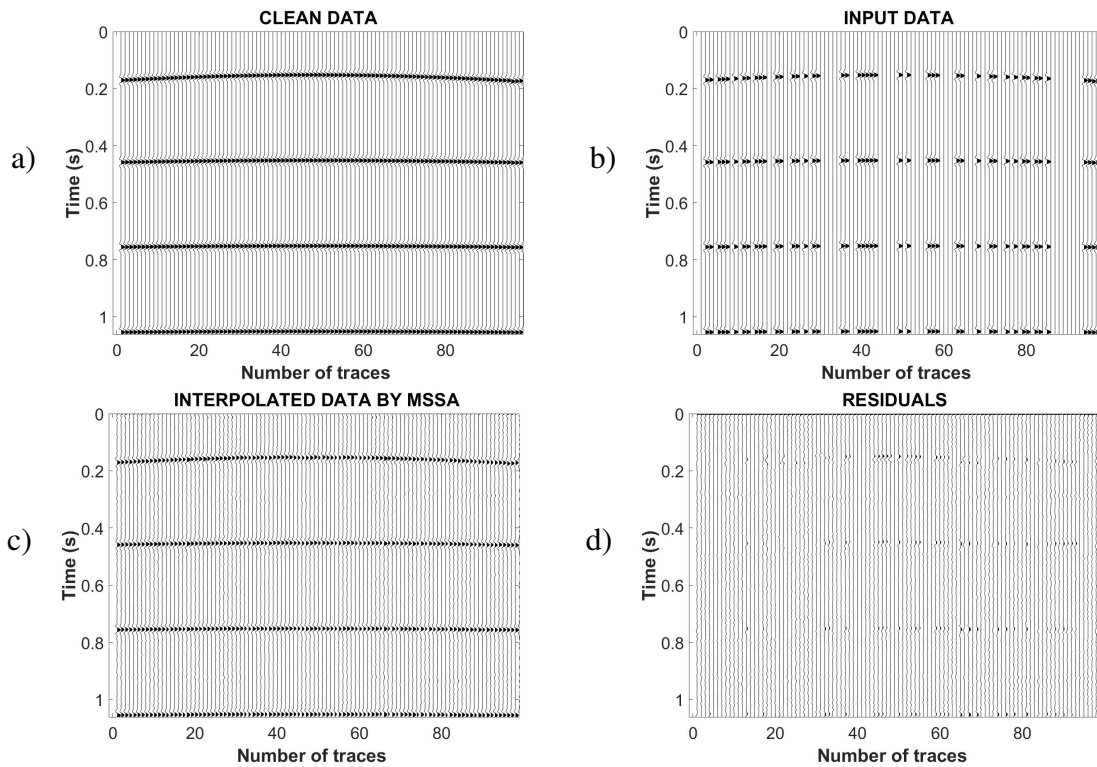


FIG. 6. Slice at $y = 5$ for the synthetic data cube. a) Initial data; b) input data with 51% randomly zeroed traces; c) interpolation result using MSSA; d) difference between (a) and (c).

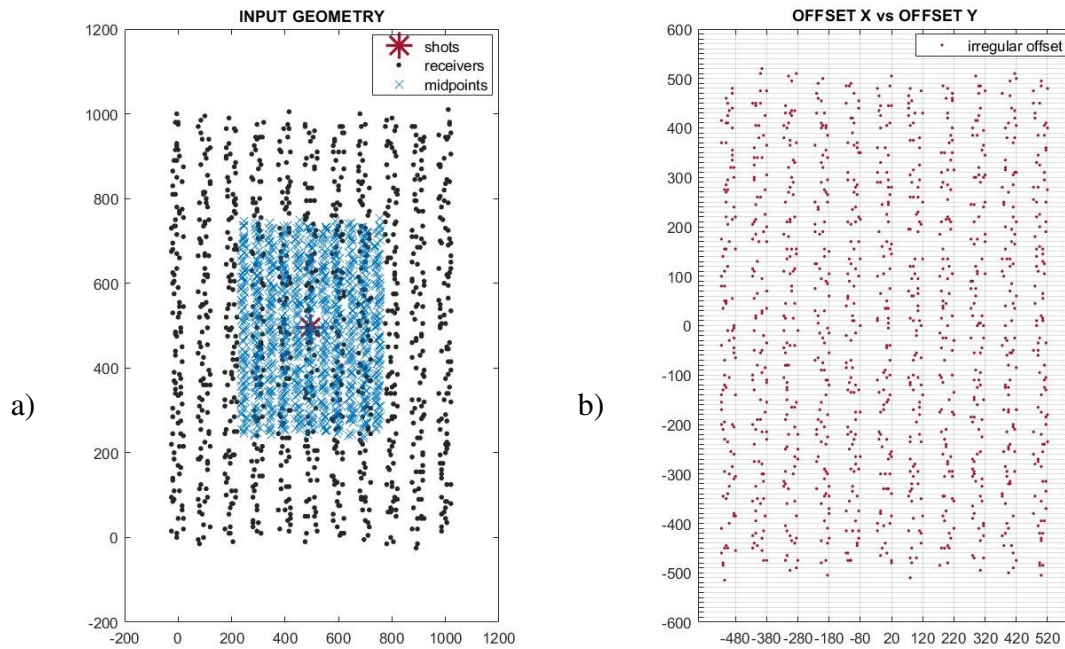


FIG. 7. a) Geometry for a synthetic shot showing shot, receiver, and midpoint locations; b) offset vector distribution.

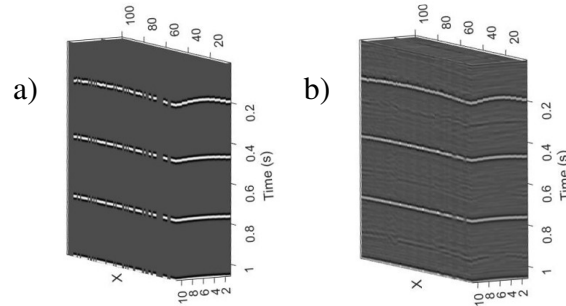


FIG. 8. Interpolation of a pre-stack synthetic cube with irregular offsets. a) Input data with a bin size of $100 \times 10 \text{ m}$; b) result of MSSA interpolation.

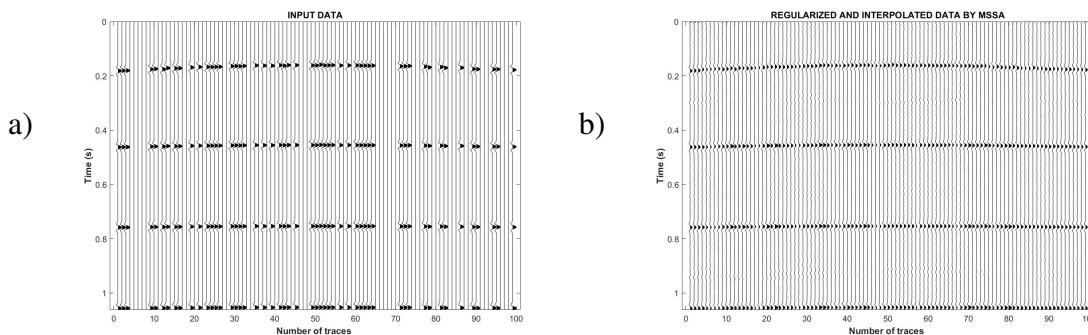


FIG. 9. a) A slice of the 3D cube at $y=5$ regularized to a bin size of $100 \times 10 \text{ m}$; b) interpolated data by MSSA.

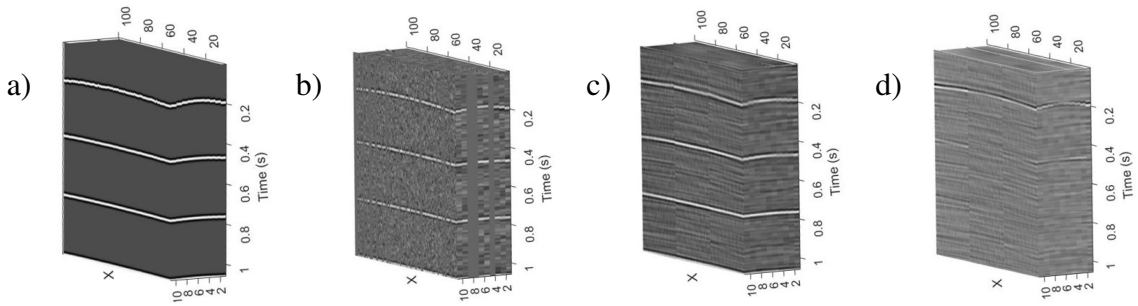


FIG. 10. Interpolation of a pre-stack synthetic cube. a) Initial data; b) input data with 31% randomly eliminated traces; c) result of the MSSA interpolation; d) difference between the result and the initial data.

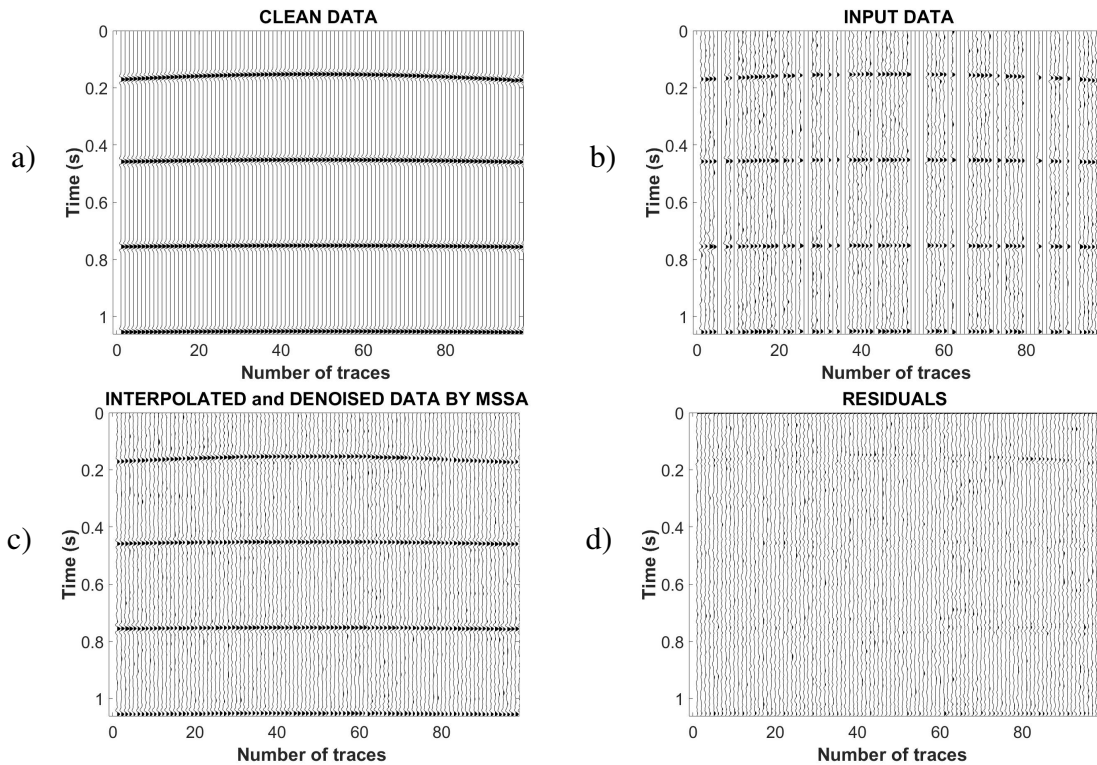


FIG. 11. A slice of the noisy 3D cube at $y=2$. a) Expected data; b) input data with 31% randomly missing traces and contaminated with random noise; c) result of the simultaneous interpolation and denoising using MSSA; d) difference between the result and expected data.

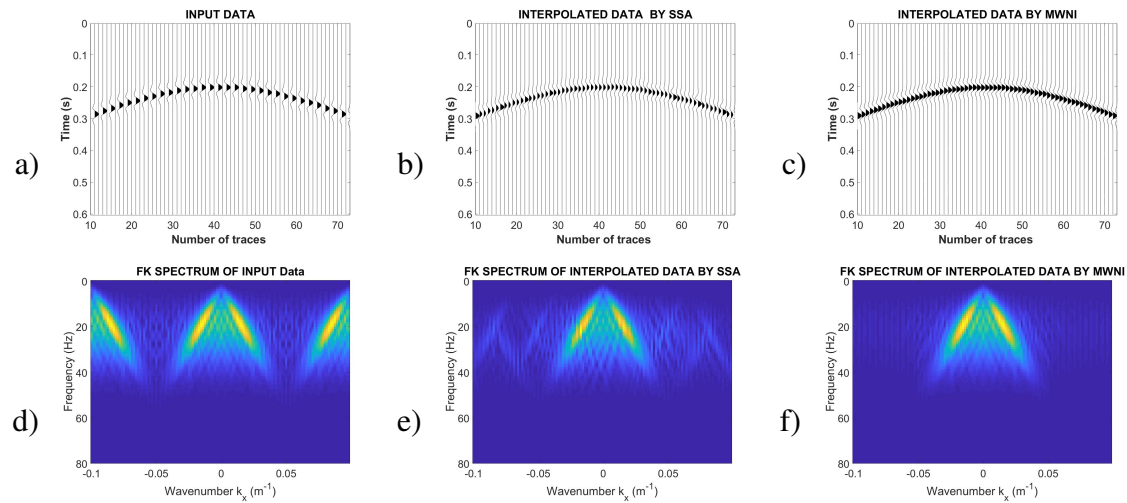


FIG. 12. Comparison between SSA and MWNI algorithms applied on 2-D pre-stack synthetic data with regularly decimated traces. a) Input data with regularly decimated traces; b) SSA interpolation result; c) MWNI interpolation result. d) the $f - k$ spectrum of input data; e) the $f - k$ spectrum of the result of SSA algorithm; f) the $f - k$ spectrum of the result of MWNI algorithm.